Available online at www.jourcc.com

Journal homepage: www.JOURCC.com

Journal of Composites and Compounds

Effects of Mg and MgO Nanoparticles on Microstructural and Mechanical Properties of Aluminum Matrix Composite Prepared via Mechanical Alloying

Behnam Nazerian Khozani [a], Aliasghar Abuchenari [a]*

[a] *Department of Material Science and Engineering, Shahid Bahonar University of Kerman, Kerman, Iran*

A B S T R A C T

Aluminum-based composites reinforced with ceramic particles have been used for many applications because of their high hardness, good wear resistance, low weight, and low thermal expansion coefficient. The Al-MgO/Mg composite was prepared in the present study. The effects of milling time and amounts of initial Mg and MgO were studied on the properties of the composite. The milled powder mixtures were subsequently analyzed by the XRD and SEM tests. Crystal sizes and internal strains were calculated using XRD data and the Williamson-Hall equation. The hardness of samples was measured by the Vickers method. The results showed that the lattice parameter significantly increased by increasing the amount of Mg. During the milling, the crystallite size, and simultaneously internal strain and hardness increased by increasing amounts of Mg and MgO. The results also showed that the effects of Mg on the composite properties were higher than MgO particles.

Peer review under responsibility of JCC Research Group

A R T I C L E I N F O R M A T I O N

Article history:
Received 21 March 2021
Received in revised form 19 May 2021
Accepted 06 June 2021

Keywords:
Composite
Mechanical alloying
Mg and MgO particles
Hardness
Sintering

1. Introduction

Metal matrix composites (MMCs) are now widely used in modern engineering applications due to their superior mechanical properties such as fracture toughness, specific stiffness to weight ratio, impact and high creep resistance, and high oxidation and corrosion resistance compared to conventional materials. MMCs with various matrix metals, such as copper, aluminum, nickel, and iron, are reinforced with various ceramics particles, such as MgO, TiC, Al_2O_3, and SiC, to increase strength through multiple strengthening mechanisms at room temperature. These include the fabrication of thermal dislocations due to a mismatch in the composite thermal expansion coefficients and the addition of refinement crystallite to the matrix microstructure [1-3].

There is an increasing demand for aluminum matrix composites reinforced with nano-ceramic particles. Because of its excellent combination of properties, such as high stiffness, low density, reasonable wear, controlled thermal expansion coefficient, and corrosion resistance, it is currently used in various applications, including aerospace and the automobile industry. Several parts are used in tribological systems in many application sectors, requiring friction performance and improved wear of these composites, thus, the addition of graphite particulates is required to improve machinability and wear resistance [4-6].

Squeeze casting, stir casting, liquid metal infiltration, powder metallurgy, mechanical alloying, and spray decomposition are some of the techniques used to make MMCs [7, 8]. In addition, mechanical alloying/milling has proved to be a successful method for improving reinforcement distribution throughout the matrix [9, 10].

Some studies have shown that reinforcements, such as SiC particles and other particles, can be successfully incorporated into an aluminum matrix using the MA technique. In addition, the refinement of sub-grain size and the uniform distribution of reinforcement have improved the properties of composites [9, 11, 12]. Moreover, nanocomposite powders made by Al-alloy powders and mechanical alloying of ceramic particles can be employed to make composites with better characteristics. Additionally, reducing the inter-particle spacing and incorporating ultrafine particles, such as nanoparticles, into the matrix improves mechanical properties significantly [13, 14].

Fine particles, on the other hand, have a higher tendency to agglomerate together. As a result, the optimum particle size, amount of reinforcement, and processing parameters should be determined for each technique and matrix [15, 16]. MgO is a better choice for reinforcement because of its high melting point (Tm = 2800 C), compressive strength, hardness, and excellent thermodynamic stability [17, 18].

According to Azhar et al., the addition of MgO particles improved the mechanical properties [19]. In addition, Abdizadeh et al. [20] demonstrated that adding fine MgO particles to Zirconia Toughened Alumina (ZTA) improved wear performance by 50% and increased hardness. Vickers hardness decreases and increases with coarser and finer MgO particle sizes, respectively, when using ZTA. Thus, the hardness of the composite specimens increases as MgO increases, while the resistance

* *Corresponding author: Aliasghar Abuchenari; E-mail:aliab596@yahoo.com*
DOR: 20.1001.1.26765837.2021.3.7.1.6
https://doi.org/10.52547/jcc.3.2.2

decreases [21]. Aluminum alloy (A356.1) matrix composites reinforced with nanoparticle MgO were fabricated using the stir casting method by Ansary yar et al. [22]. According to the findings, the composites with 1.5 vol. % reinforcement particles fabricated at 850 °C had a homogeneous microstructure and improved mechanical properties.

This research aims to investigate the impact of MgO and Mg nanoparticle content on mechanical properties and the microstructure of Al-MgO/Mg composites made by mechanical alloying, along with the effect of MgO and Mg content on the crystal parameters.

2. Materials and methods

2.1. Materials

Pure aluminum powder (99 wt%), pure magnesium powder (99 wt%), and pure magnesium oxide powder (98 wt%) were purchased from Khorasan Powder Metallurgy Co. (Mashhad, Iran). The particle sizes of Al, MgO, and Mg powder were 25, 120, and 136 μm, respectively.

2.2. Composite preparation

Aluminum metal matrix composites were prepared by a mechanical alloying technique. In the first step, the pure aluminum powder reinforced with 5 wt% of MgO powder was produced by ball milling with the following parameters: ball-to-powder weight ratio: 20:1, ball diameter: 1 and 2 cm, ball material: AISI 420 quenched stainless steel, and speed 250 rpm. Ethanol 3% (wt.) was added to control the process. The argon atmosphere was also used as a control gas. Then, pure aluminum powder with a constant content of MgO powder (5 wt%) was reinforced with 10 and 15 wt% of Mg powder. In the last step, pure aluminum powder with a constant content of Mg powder (10 wt%) was reinforced with 10 and 15 wt% of MgO powder. The powder was cold-pressed (pressure: 25.4 MPa) in a steel mold. The compressed samples were then sintered in a furnace (Shenyang GE Furnace Co. LTD, Shenyang, China) with argon atmosphere at 400°C for 45 min. These samples were produced to investigate the effects of MgO and Mg on the microstructure and mechanical properties of the metal matrix composite. The sample balls were milled for 5, 10, 20, and 40 h because the time was necessary to complete the mechanical alloying process. Finally, the composites were obtained with these compounds: Al-5MgO, Al-5MgO/10Mg, Al-5MgO/15Mg, Al-10MgO/10Mg, and Al-15MgO/10Mg.

2.3. Characterization and testing

The composites were subjected to the X-Ray diffraction (XRD) analysis. Crystalline phases were identified using X'Pert HighScore software (2.2b) equipped with the PCPDFWIN database.

Crystallite size and lattice-strain were determined by the Hall-Williamson method [23]:

$$\beta\cos\theta = 2\varepsilon\sin\theta + \frac{0.9\lambda}{D}$$

where "B" is broadening due to crystallite size and lattice strain, is strain, "θ" is the 'Bragg's angle, "λ" is the wavelength of the incident X-ray beam in nm, and "D" is crystalline size. Lattice strains were identified by Sigma Plot software.

Equation 3-2 [24] also determines lattice parameters:

$$a = \frac{\lambda\sqrt{h^2+k^2+l^2}}{2\sin\theta}$$

The lattice parameters were determined for (2 2 0), (3 1 1), and (2 2 2) and the extrapolation function method.

The microstructure of the samples was analyzed by a Scanning Electron Microscope (SEM, JEOL JSM-5800 LV) with energy-dispersive X-ray spectroscopy (EDX) at an operating voltage of 20 kV, and the particle size was determined with Image Tools software. The hardness of the composites was evaluated by the Micro–Vickers hardness tester (Struers, Durmin20). The mean of five measurements was recorded in various regions of the polished samples. The applied load and the time of loading were 250 mN and 5s, respectively.

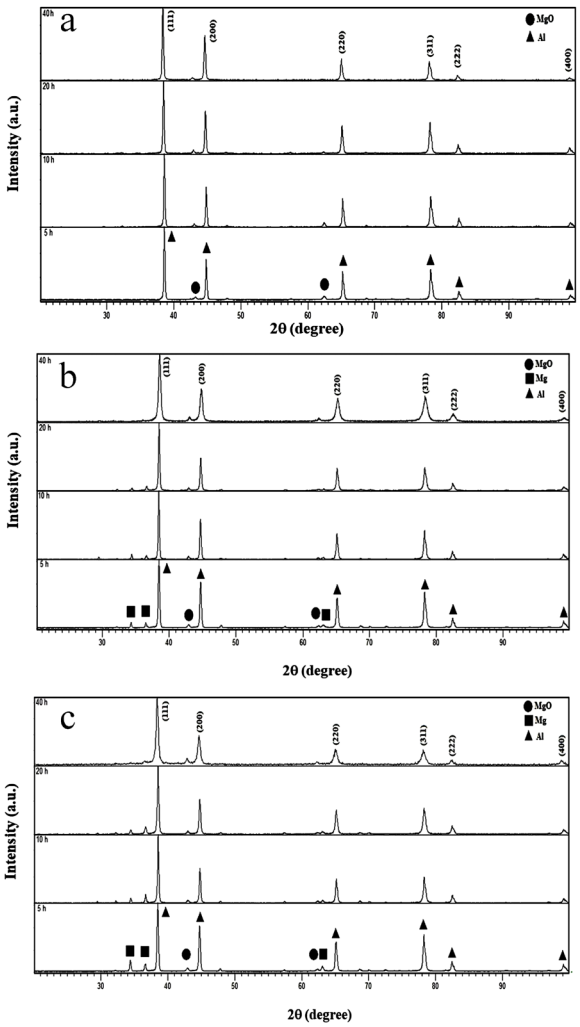

Fig. 1. X-ray diffraction pattern of composites in various times of ball milling. a) Al-5MgO composite, b) Al-5MgO/10Mg composite, and c) Al-5MgO/15Mg composite. .

3. Results and discussion

3.1. XRD analysis

Figure 1 shows the X-ray diffraction pattern of the prepared composites with various amounts of Mg nanoparticles. Figure 1-a shows the XRD pattern of the Al-5MgO composite at various times of ball milling. Aluminum peaks with a high height and low width with an FCC crystal structure, as well as MgO peaks, can be seen in the first 5 h. The aluminum peaks become wider and their height decreases as the milling time increases to 40 h. In addition, the non-displacement of aluminum peaks is observed during milling, and the peaks related to MgO in the diffraction pattern of the powder mixture are shortened over time while studying the diffraction angle of aluminum peaks.

There is no solid solution formed because MgO particles do not enter the aluminum lattice. The peak of MgO particles does not disappear because they do not dissolve in the aluminum lattice. However, as milling time increases, the size of magnesium oxide particles decreases below microns, causing them to appear less intense on the XRD. The mech-

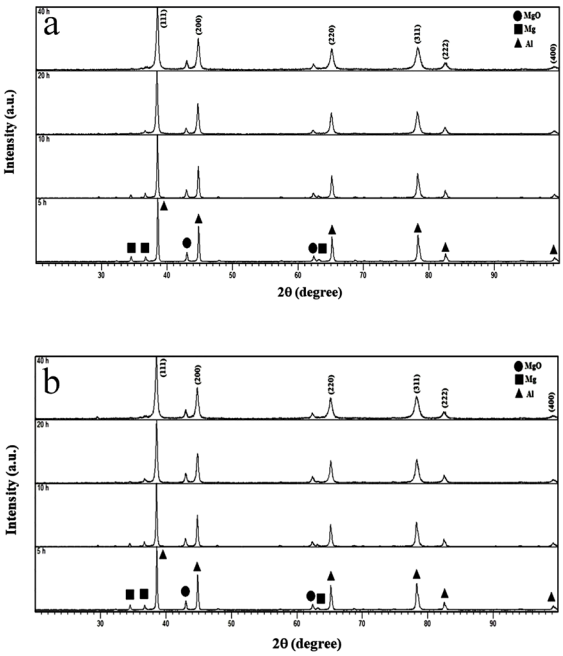

Fig. 2. X-ray diffraction pattern of composites at various times of ball milling. a) Al-10MgO/10Mg composite and b) Al-15MgO/10Mg composite.

anism is that magnesium oxide particles crush and distribute the underlying powder among the aluminum particles, changing its behavior. High-energy collisions of bullet-powder-bullet and bullet-powder-container create many crystal defects in the milling process, such as borders, misalignments, and voids, which increase over time. The ground lattice parameter does not increase because magnesium oxide particles enter the aluminum field, implying no diffusion mechanism [24, 25].

Figures 1-b and 1-c show the XRD patterns of Al-5MgO/10Mg and Al-5MgO/15Mg composites at various ball milling times. All peaks related to aluminum with FCC crystal structure, magnesium with HCP crystal structure, and magnesium oxide peaks can be seen for both samples in the first 5 h. The intensity of magnesium peaks gradually decreased with increasing milling time from 5 to 20 h but did not completely disappear. The magnesium peak was completely disappeared after 40 h of milling, leaving only the aluminum peaks with FCC structures and magnesium oxide. Aluminum peaks also shifted towards lower diffraction angles. Clearer small Mg peaks are seen in the dispersion pattern of the primary powders in the mixture containing 15% by weight of magnesium (Fig. 1-c) and fade away over milling time, indicating that the magnesium particles in the aluminum field are dissolved during the mechanical alloying process. The formation of solid-aluminum-magnesium supersaturated solution with FCC structure in mechanical alloying of powdered aluminum and magnesium has been reported by Gubicza [26], Umbrajkar [27], Scudino [28], Singh [29], Aqeeli [30, 31], and Youssef [32]. The absence of peaks in XRD patterns related to compounds between aluminum and magnesium, on the other hand, could be a reason for magnesium solubility in aluminum. These findings, combined with previous findings, show the formation of (Al(Mg)ss) without the formation of metal-metal compounds of up to 30% of magnesium atoms. It is in agreement with [27-29, 31, 33] that the solubility of the alloying elements, the presence of stress in the microstructure, and crystallite shrinkage have all been blamed for the increase in the width of the aluminum peaks [34].

According to the examination, the intensity of the aluminum peaks decreased and their width increased during milling in all three samples. The figures also show that as the magnesium percentage increases, the peaks become wider and their intensity decreases, indicating an increase in the lattice strain and a decrease in the crystallite size with the increased magnesium content.

Figure 2 shows the XRD pattern of the prepared composites with various amounts of MgO nanoparticles. Figure 2 (a and b) shows the XRD patterns of Al-10MgO/10Mg and Al-15MgO/10Mg composites at various times of ball milling.

The XRD pattern variations of these two samples are approximately similar to that of the Al 5MgO/10Mg sample. As the milling time increases, the peak intensity of magnesium with an HCP structure also decreases and gradually disappears. It is also observed that as the milling time increases, the aluminum peaks become wider and their intensity decreases. Finally, aluminum peaks with the FCC structure and magnesium oxide are seen after 40 h of milling. It is also observed that the peaks become wider and their height decreases with increasing the milling time, which indicates an increase in the lattice strain and a decrease in the crystallite size with increasing the milling time [33].

3.2. Crystallite size and lattice characteristics

Graphs of crystallite size, lattice strain, and lattice parameter size in terms of milling time for different chemical compounds are shown in Figure 3 (a-c). Figure 3-a shows the crystallite size diagram in terms of milling time for different chemical compositions, indicating that the crystallite size decreases with increasing milling time. The process of reducing the crystallite size to 40 h is nearly identical with the addition of magnesium and the increased milling time. Crystallite size decreases on a steep slope in the early stages of milling, and milling is then done at a slower rate, between 20 and 40 h. Al-5MgO, for example, reduces the crystallite size to 54 nm when the milling time is increased to 40 h. The figure also shows that the decrease in crystallite size becomes more significant as magnesium increases up to 15% by weight after 40 h of milling. Al/5MgO composite powder reduces the crystallite size of this composite from 54 to 26 nm. The crystallite size decreases by a significant slope when magnesium oxide is added to Al-(5-15) MgO/10Mg composites and the fine-crystallite decreases at a much slower rate when the milling time is increased from 5 to 20 h. The crystallite size of all three samples became nearly identical in 40 h, ranging from 32 to 37 nm. It is clear from this graph that the effect of various amounts of MgO is less than that of Mg. In general, as milling time increases, severe plastic deformation in powder particles increases crystalline defects such as spot defects, misplacements, and so on [35-37].

The presence of crystal defects increases the system energy and increases the lattice strain. To compensate for the effect mentioned above, the system misplaces sub-crystallites with a less energetic arrangement, and eventually, the sub-crystallites become the main crystallites due to the mechanical work by rotating the sub-crystallites and sliding the crystallite boundaries, which causes micro-crystallinity and the formation of a nanocrystalline structure during the mechanical alloying process [26, 35, 36, 38].

Figure 3-b shows the lattice strain diagram in terms of milling time for various chemical compounds, depicting an increase in the Al-5MgO sample lattice strain at a relatively constant rate. However, the lattice strain increases more sharply as the amount of magnesium increases with decreasing crystallite size, and the rate of increase in lattice strain decreases over time. The figure also shows that as the magnesium level rises, the lattice strain rises significantly. On the other hand, it is clear from the two forms that increasing magnesium oxide by 10 and 15 wt. % does not significantly change the crystallite size or the Al-MgO/10Mg composite lattice strain. On the other hand, magnesium oxide particles are hard particles that, when placed between ground phase particles, cause a local strain around them, increasing dislocation density, thereby speeding up the fine-crystallite process. However, the effect of magnesium on the crystallite size and lattice strain is greater than that of the

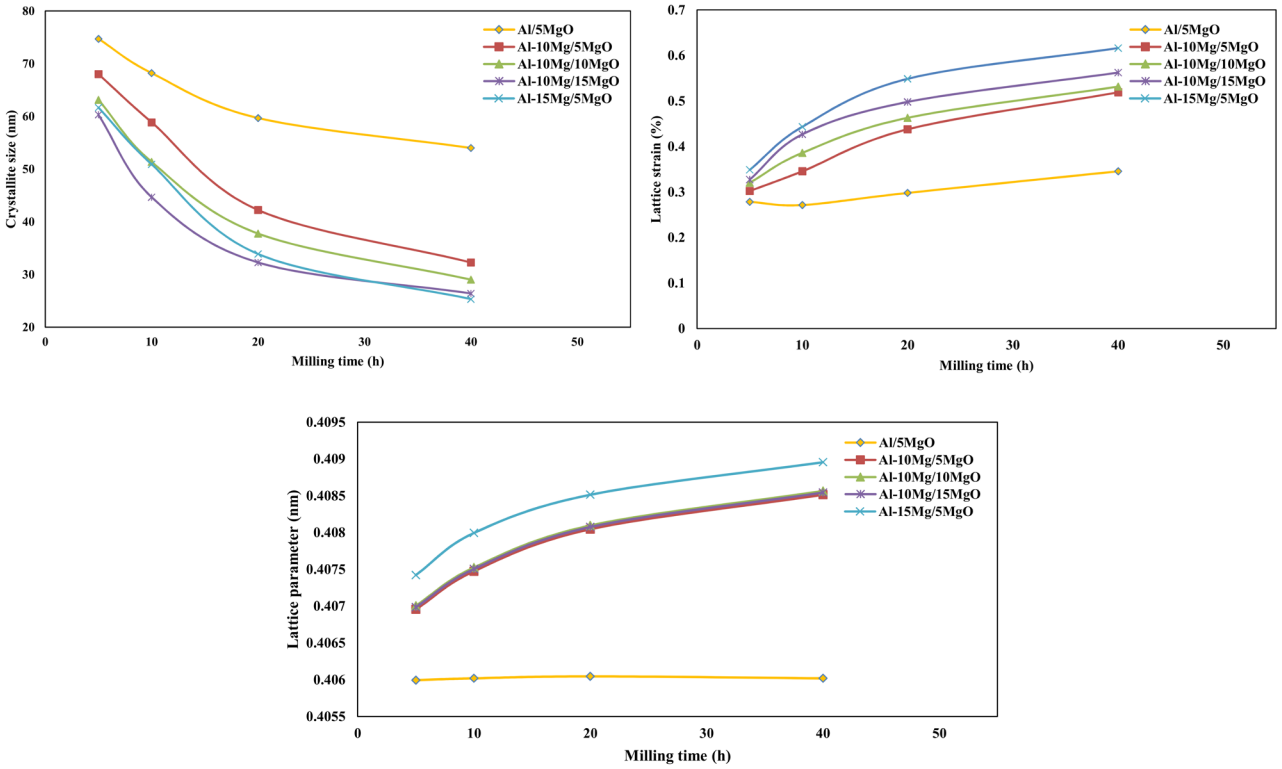

Fig. 3. The variations of composites according to ball milling times. a) Crystallite size variations, b) lattice strain variation, and c) lattice parameter variation.

magnesium oxide percentage.

Different mechanisms of MgO and Mg for increasing dislocation density can be attributed to this phenomenon. For example, MgO particles cause local strain around them and increase dislocation density by crushing and dispersing among aluminum particles, whereas Mg dissolving in aluminum causes hard work in the background powder particles and increases dislocation density during milling time. Of course, increasing the amount of magnesium oxide and crushing it, and increasing the local strain and dislocation density both accelerate the dissolution of magnesium in the aluminum field [4, 15]. Similarly, the increasing effect of Al_2O_3 reinforcing particles by 5, 10, and 15 wt.% on the microstructure of Al-10Mg/Al_2O_3 composites were reported in a study by Safari [39]. Their findings revealed that increasing the number of Al_2O_3 particles did not result in a significant decrease in crystallite size or an increase in the lattice strain.

Figure 3-c shows the size of the lattice parameter in milling time for different percentages of magnesium and magnesium oxide. The crystallite parameter for the Al-5MgO sample has a constant value with increasing the milling time, as shown in the figure. The figure also shows that as the magnesium increases, the lattice parameter increases significantly. For Al-(5-15)MgO/10Mg composites, changes in the lattice parameters with the addition of magnesium oxide are not noticeable over time and have an almost constant trend for all three samples. Because of the saturation of soluble magnesium in aluminum at the start of milling, the increase of the aluminum lattice parameter with milling time is faster than for long periods. Therefore, the more magnesium in the powder mixture, the more changes in the aluminum lattice parameter happen, and the number of magnesium atoms increases in the aluminum field. In general, the increase in solid solubility of magnesium in aluminum during mechanical alloying is attributed to the formation of a nanocrystalline structure and the creation of a large volume fraction of crystallite boundaries [40]. The results of Gubicza [41], Youssef [40], and Scudino [42] also show an increase in the lattice parameter in aluminum-magnesium alloys with increasing magnesium content and milling time. According to Figure 3, the amplifier phase does not affect the lattice parameter because magnesium oxide does not enter the aluminum lattice. In addition, no solid solution is formed, and local strain in the aluminum field only increases by crushing and distribution in the aluminum field; besides, dislocation density causes the peak height to be shortened [43].

3.3. Microstructure analysis

The SEM images of the Al-5MgO composite powder milled at various times are shown in Figures 4(a-d). The SEM image of the sample ground for 5 h shows that the particles are severely deformed and form a flat, flaky morphology due to the impact of the soft ground powder on the pellets and the particle mill. The difference in crystallite size is very noticeable at this time. Some particles are small while others are quite large. The particles flatten and flake as the milling time is increased to 10 and 20 h, indicating the cold welding process and the flexibility of the aluminum powder. Finally, dislocation density in the particles increases after 40 h of milling and significant deformation of the powder particles, resulting in increased work hardening and brittleness in the powder particles [44].

Magnesium oxide particles are also used as reinforcements in the joints of welded metal particles, increasing the substrate hardness even more. Because of the brittleness of powder particles, they are broken by increasing their hard work, thereby decreasing the size of the powder particles. The morphology of the flat state becomes almost coaxial with the breaking of plate powder particles and the absence of cold welding, but a stable state is not created in the powder particles.

The SEM images of the Al-5MgO/10Mg and Al-5MgO/15Mg powder samples, milled at different times, are shown in Figures 5 and 6. Due to collisions between the powder particles and the particle mill container after 5 h of milling, they became wider in these samples with the addition of magnesium.

Due to the dominance of the cold welding process, the particle size

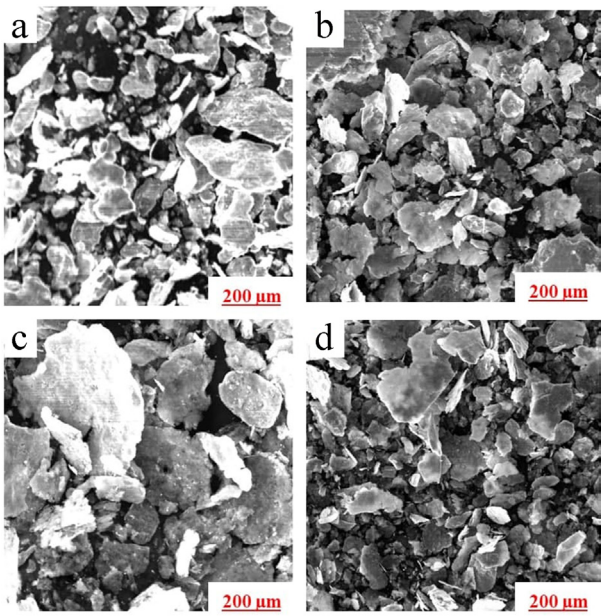

Fig. 4. SEM image of Al-5MgO sample after (a) 5, (b) 10, (c) 20, and (d) 40 h of milling.

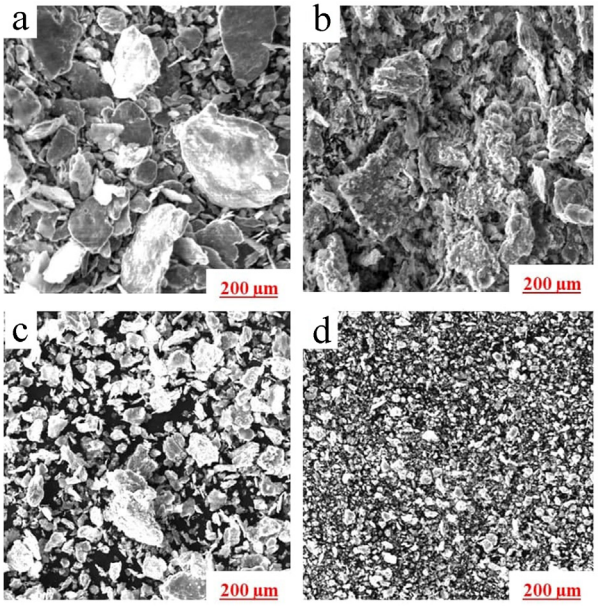

Fig. 5. SEM image of Al-5MgO/10Mg sample after (a) 5 (b) 10 (c) 20 (d) 40 hours of milling.

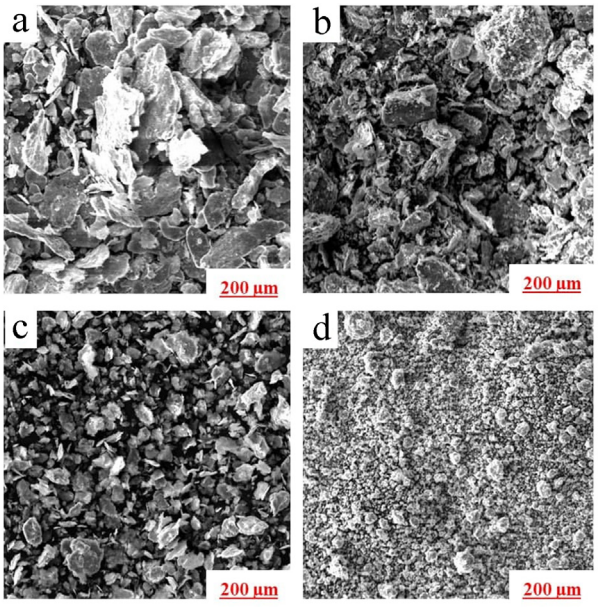

Fig. 6. SEM image of the Al-5MgO/15Mg15 sample after (a) 5 (b) 10 (c) 20 (d) 40 hours of milling.

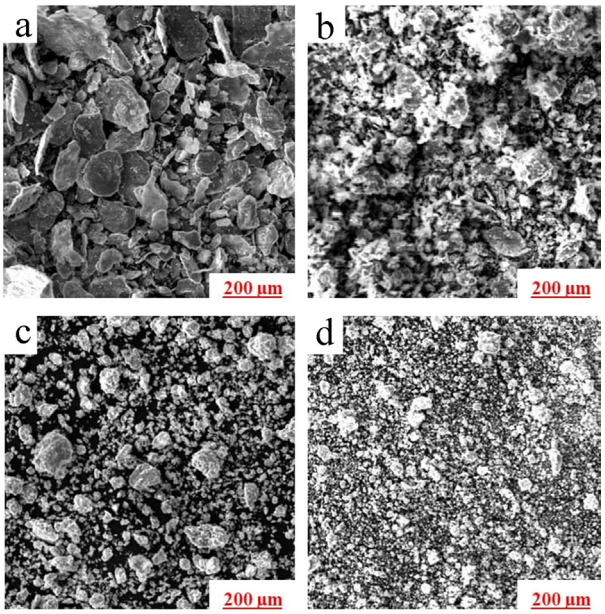

Fig. 7. SEM image of Al-10MgO/10Mg sample after (a) 5 (b) 10 (c) 20 (d) 40 hours of milling.

increases as the milling time increases to 10 h, resulting in a layered morphology of the powder particles. The structure of the layers disappears as the milling time increases from 10 to 20 h, and they are prone to failure due to the hard work created in the powder. The powders become finer, and the particle size distribution becomes more uniform as the failure process takes precedence over the cold welding process. Finally, a completely coaxial morphology with fine particles and a uniform particle size distribution is formed after 40 h of milling. Therefore, both the penetration of magnesium into the aluminum lattice and the hard work in the powder particles increases with the increase in magnesium. After 40 h of milling, the mechanical milling process is accelerated and the powder particles are in a stable state [45].

SEM images of powdered Al-10MgO/10Mg and Al-15MgO/10Mg samples taken at various times (Figs. 7 and 8) clearly show that their morphology follows a similar pattern to that of the Al-5MgO/10Mg composite using the same procedure. In addition, all three samples had a completely coaxial morphology with fine particles and a uniform particle size distribution after 40 h of milling.

Figure 9 depicts particle size with various compositions and milling times. The average particle size of Al-5MgO composite powder increases to 59 microns with an increase in milling time of up to 20 h due to the predominance of the cold-welding process. Then, it decreases to 47 microns after 40 h of milling due to the predominance of the fracture process. The average powder particle size for Al-5MgO/10Mg composite powder increases to 46 microns after 10 h and then it rapidly decreases with increasing time to 20 h. The particle size of the powder decreases at a slower rate of up to 13 microns between 20 and 40 h.

The same process can be seen in the Al-5MgO/15Mg composite powder sample, which has a particle size of 42 microns after 10 h but decreases to 9 microns after 40 h. It is also known that both the maximum particle size of the powder and the time required to achieve that size decrease as magnesium intensity increases, implying that magnesium speeds up the mechanical milling process. Finally, the steady-state, i.e., the balance between the two processes of cold-welding and failure in the powder particles is not achieved and the particle size decrease trend continues after 40 h of milling. As a result, the milling operation must be

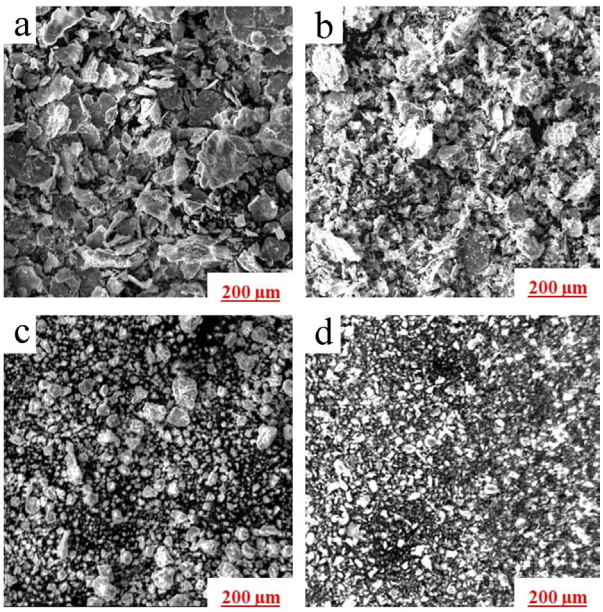

Fig. 8. SEM image of Al-15MgO/10Mg sample after (a) 5 (b) 10 (c) 20 (d) 40 hours of milling.

carried out over a longer period to achieve a stable state.

The particle size changes of Al-(5-15)MgO/10Mg composite powders follow a nearly identical pattern in this diagram, and the maximum particle size decreases with the addition of magnesium oxide. It is also known that as the amount of magnesium increases in the powder, the particle size of the powder decreases so does the time it takes to reach the maximum particle fineness. The amount of magnesium has also been found to reduce the maximum particle size. Consequently, the effect of increasing magnesium is more pronounced than that of increasing magnesium oxide, as shown in this graph. This phenomenon can be explained by the different effects of MgO and Mg on the behavior of powders. MgO particles change the behavior of the powder by crushing and dispersing it among the aluminum particles, whereas Mg dissolving in the aluminum background during milling changes the behavior of the composite powder [15, 45].

3.4. hardness test

Figure 10-a shows changes in the microhardness of composite powders with milling time before heat treatment. As the magnesium level rises, the hardness level rises as well. It is also known that an increase in magnesium has a greater effect on the hardness of the samples than that in magnesium oxide. With an increase in the milling time of up to 40 h, the microhardness of Al-5MgO composite powder increases with a relatively constant trend of up to 165 V. Increasing the milling time to 40 h causes more hard work in the ground powder particles and leads to the breaking of brittle and large MgO particles and even the distribution of the particles in the aluminum field. This increases dislocation density, increasing the hard work on the powder particles even more.

The hardness of the Al-5MgO composite increases significantly by are adding 10% and 15% magnesium, to the point where the microhardness values of the Al-5MgO/10Mg and Al-5MgO/15Mg composite samples increase to 208 and 236, respectively. The increase in microhardness of up to 20 h is attributed to magnesium dissolution in the aluminum field, as well as an increase in dislocation density and hard work in the powder particles.

The solubility of magnesium in the field of aluminum increases as the percentage of magnesium increases, and so does the work hardening and dislocation density. On the other hand, increasing both the percentage of magnesium and the milling time by more than 20 h causes the dislocation density to increase, dynamic recovery to occur, and hardening speed to decrease due to increased work hardening. The formation of a solid solution (Al(Mg)ss) and the intensification of hardness due to the presence of soluble magnesium in the aluminum are two mechanisms by which magnesium increases hardness. Figure 10 shows that while increasing the percentage of MgO to 10 and 15 wt.% causes a slight increase in hardness, it is not significant. Al-10MgO/10Mg and Al-15MgO/10Mg composites have microhardness values of 215 and 220 Vickers after 40 h, respectively. The different mechanisms of the two for increasing hardness are attributed to the low effect of magnesium oxide particles on magnesium [15, 45, 46]. Figure 10-b shows changes in the microhardness of composite powders with milling time after heat treatment. After sintering, the hardness of all samples decreases, with the magnesium-free sample having the lowest hardness, indicating the occurrence of the recovery and recrystallization processes, lowering the work hardness of the powder particles. For example, without magnesium, hardness drops by about 30%, while increases of 10% and 15% by weight result in hardness drops of about 16 and 9%, respectively. The hardness of the sample without magnesium decreases as recovery and recrystallization processes occur, and the hardness reduction levels were about 11 and 10%, respectively, when magnesium oxide was increased by 10% and 15% by weight.

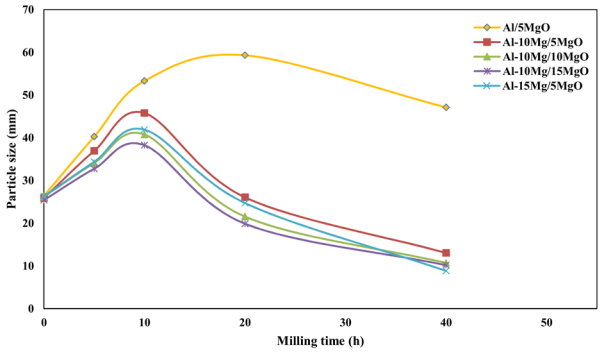

Fig. 9. Changes in particle size according to various compositions and milling times.

Despite the recovery and recrystallization processes, two factors prevented the reduction of hardness in the magnesium-containing sample. First, it slows down the game, but it also makes it more difficult. On the other hand, as the number of magnesium oxide particles increases, the amount of work required increases, causing these particles to decrease and, as a result, the dislocation density to rise. The penetration process is accelerated, and the probability of magnesium dissolving increases in the aluminum field, which increases the hardness of the samples and compensates for the decrease in post-sintering hardness by increasing the dislocation density during sintering [20].

4. Conclusions

At different milling times, adding magnesium to Al/MgO composite powder reduces crystallite size and increases composite lattice strain. Magnesium is dissolved into aluminum and forms an aluminum-magnesium supersaturated solid solution (Al (Mg) ss) when magnesium is added to the Al/MgO composite powder, increasing the composite lattice parameter. In Al/5MgO composite powder, increasing the magnesium percentage leads to a coaxial morphology with finer particle size and more uniform distribution. The increase in the amount of dissolved magnesium in the aluminum field and the change in its mechanical behavior are the causes of these changes. Before sintering, the hardness of the samples increases as milling time and magnesium increase. The hardness drops after the sintering process in the sample without magnesium

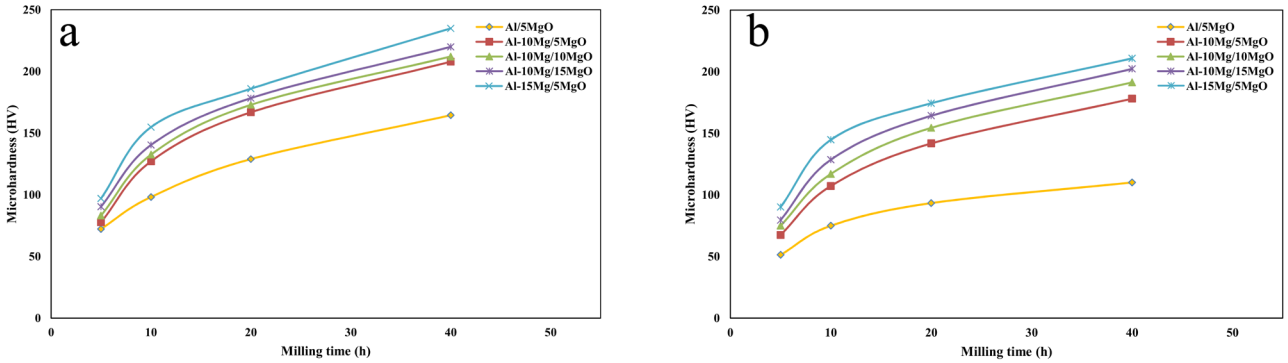

Fig. 10. a) Micro-hardness changes of different powder samples according to pre sintering milling time b) Micro-hardness changes of different powder samples according to post sintering milling time (at 400 °C for 45 minutes).

due to the recovery and recrystallization processes. As the magnesium content increases, the soluble magnesium in the recovery and recrystallization processes slows down and eventually stops, reducing the hardness drop. The effect of increasing magnesium oxide on decreasing crystallite size, increasing underlying lattice strain, morphological changes, powder particle size, and sample hardness (before and after sintering) is more negligible than increasing magnesium.

Acknowledgments

The authors would like to acknowledge Shahid Bahonar University of Kerman for the financial support towards this research.

Conflict of interest

The authors declare that there is no conflict of interest.

REFERENCES

[1] S. Bahl, Fiber reinforced metal matrix composites-a review, Materials Today: Proceedings 39 (2021) 317-323.
[2] K.U. Kainer, Basics of metal matrix composites, Metal Matrix Composites (2006) 1-54.
[3] N. Manikandan, K. Balasubramanian, D. Palanisamy, P. Gopal, D. Arulkirubakaran, J. Binoj, Machinability analysis and ANFIS modelling on advanced machining of hybrid metal matrix composites for aerospace applications, Materials and Manufacturing Processes 34(16) (2019) 1866-1881.
[4] S.S. Irhayyim, H.S. Hammood, A.D. Mahdi, Mechanical and wear properties of hybrid aluminum matrix composite reinforced with graphite and nano MgO particles prepared by powder metallurgy technique, AIMS Mater Sci 7 (2020) 103-115.
[5] Casati, Aluminum Matrix Composites Reinforced with Alumina Nanoparticles, first ed, Springer International Publishing, Cham, Switzerland 2016 pp. 9-15.
[6] M. Tayyebi, D. Rahmatabadi, R. Hashemi, Review of mechanical and microstructural properties of aluminum matrix composites reinforced with ceramic particles produced by SPD processes, Journal of Science and Technology of Composites 5(4) (2019) 583-594.
[7] M.N.E. Efzan, N.S. Syazwani, A.M.M. Al Bakri, Fabrication Method of Aluminum Matrix Composite (AMCs): A Review, Key Engineering Materials 700 (2016) 102-110.
[8] A.K. Sharma, R. Bhandari, C. Pinca-Bretotean, A systematic overview on fabrication aspects and methods of aluminum metal matrix composites, Materials Today: Proceedings 45 (2021) 4133-4138.
[9] C.-Z. Nie, J.-J. Gu, J.-L. Liu, D. Zhang, Production of boron carbide reinforced 2024 aluminum matrix composites by mechanical alloying, Materials Transactions 48(5) (2007) 990-995.
[10] K.R. Cardoso, B.d.S. Izaias, L.d.S. Vieira, A.M. Bepe, Mechanical alloying and spark plasma sintering of AlCrCuFeZn high entropy alloy, Materials Science and Technology 36(17) (2020) 1861-1869.
[11] M. Adamiak, Mechanical alloying for fabrication of aluminium matrix composite powders with Ti-Al intermetallics reinforcement, Journal of Achievements in Materials and Manufacturing Engineering 31(2) (2008) 191-196.
[12] D. ŞİMŞEK, İ. SİMSEK, D. ÖZYÜREK, Production and Characterization of Al-SiC Composites by Mechanical Milling, Bitlis Eren Üniversitesi Fen Bilimleri Dergisi 8(1) (2019) 227-233.
[13] R. Pandiyarajan, M. Prabakaran, T. Rajkumar, K.V. Kumar, R. Manikandan, Metallurgical and mechanical properties of SiC/B_4C reinforced with aluminum composites synthesized by mechanical alloying, Materials Today: Proceedings 37 (2021) 1794-1798.
[14] H. Arik, Effect of mechanical alloying process on mechanical properties of α-Si_3N_4 reinforced aluminum-based composite materials, Materials & Design 29(9) (2008) 1856-1861.
[15] A.A. Yar, M. Montazerian, H. Abdizadeh, H. Baharvandi, Microstructure and mechanical properties of aluminum alloy matrix composite reinforced with nano-particle MgO, Journal of Alloys and Compounds 484(1-2) (2009) 400-404.
[16] V. Chak, H. Chattopadhyay, T. Dora, A review on fabrication methods, reinforcements and mechanical properties of aluminum matrix composites, Journal of Manufacturing Processes 56 (2020) 1059-1074.
[17] K. Joshua, V. Santhiyagu, P.S. Dirviyam, P. Ramkumar, Influence of MgO particles on Microstructural and Mechanical Behaviour of AA7068 Metal Matrix Composites, IOP Conference Series: Materials Science and Engineering 247 (2017) 012011.
[18] H. Abdizadeh, P. Vajargah, M. Baghchesara, Fabrication of MgO nanoparticulates reinforced aluminum matrix composites using stir-casting method, Kovove Mater 53 (2015) 319-326.
[19] A.Z.A. Azhar, H. Mohamad, M.M. Ratnam, Z.A. Ahmad, The effects of MgO addition on microstructure, mechanical properties and wear performance of zirconia-toughened alumina cutting inserts, Journal of alloys and compounds 497(1-2) (2010) 316-320.
[20] H. Abdizadeh, R. Ebrahimifard, M.A. Baghchesara, Investigation of microstructure and mechanical properties of nano MgO reinforced Al composites manufactured by stir casting and powder metallurgy methods: A comparative study, Composites Part B: Engineering 56 (2014) 217-221.
[21] M. Em Pul, R. Calin, F. Gül, Investigation of abrasion in Al–MgO metal matrix composites, Materials Research Bulletin 60 (2014) 634-639.
[22] A.A. Yar, M. Montazerian, H. Abdizadeh, H.R. Baharvandi, Microstructure and mechanical properties of aluminum alloy matrix composite reinforced with nano-particle MgO, Journal of Alloys and Compounds 484(1) (2009) 400-404.
[23] G. Williamson, W. Hall, X-ray line broadening from filed aluminium and wolfram, Acta Metallurgica 1(1) (1953) 22-31.
[24] R. Wahab, S.G. Ansari, M.A. Dar, Y.S. Kim, H.S. Shin, Synthesis of Magnesium Oxide Nanoparticles by Sol-Gel Process, Materials Science Forum 558-559 (2007) 983-986.
[25] M.A. Baghchesara, H. Abdizadeh, Microstructural and mechanical properties of nanometric magnesium oxide particulate-reinforced aluminum matrix composites produced by powder metallurgy method, Journal of mechanical science and technology 26(2) (2012) 367-372.
[26] J. Gubicza, M. Kassem, G. Ribárik, T. Ungár, The microstructure of mechanically alloyed Al–Mg determined by X-ray diffraction peak profile analysis, Materials Science and Engineering: A 372(1-2) (2004) 115-122.
[27] S.M. Umbrajkar, M. Schoenitz, S.R. Jones, E.L. Dreizin, Effect of temperature on synthesis and properties of aluminum–magnesium mechanical alloys, Journal of Alloys and Compounds 402(1) (2005) 70-77.
[28] S. Scudino, M. Sakaliyska, K.B. Surreddi, J. Eckert, Mechanical alloying and milling of Al–Mg alloys, Journal of Alloys and Compounds 483(1) (2009) 2-7.
[29] D. Singh, C. Suryanarayana, L. Mertus, R.H. Chen, Extended homogeneity range of intermetallic phases in mechanically alloyed Mg–Al alloys, Intermetallics

11(4) (2003) 373-376.
[30] N. Al-Aqeeli, G. Mendoza-Suarez, A. Labrie, R.A.L. Drew, Phase evolution of Mg–Al–Zr nanophase alloys prepared by mechanical alloying, Journal of Alloys and Compounds 400(1) (2005) 96-99.
[31] N. Al-Aqeeli, G. Mendoza-Suarez, C. Suryanarayana, R.A.L. Drew, Development of new Al-based nanocomposites by mechanical alloying, Materials Science and Engineering: A 480(1) (2008) 392-396.
[32] K.M. Youssef, R.O. Scattergood, K. Linga Murty, C.C. Koch, Ultratough nanocrystalline copper with a narrow grain size distribution, Applied physics letters 85(6) (2004) 929-931.
[33] A. Wagih, Mechanical properties of Al–Mg/Al_2O_3 nanocomposite powder produced by mechanical alloying, Advanced Powder Technology 26(1) (2015) 253-258.
[34] B.D. Cullity, Elements of X-ray Diffraction, Addison-Wesley Publishing, USA 1956.
[35] C. Suryanarayana, M.G. Norton, X-Ray Diffraction: A Practical Approach, Springer US, USA 1998.
[36] Y. Saberi, S.M. Zebarjad, G.H. Akbari, On the role of nano-size SiC on lattice strain and grain size of Al/SiC nanocomposite, Journal of Alloys and Compounds 484(1) (2009) 637-640.
[37] C. Suryanarayana, Mechanical alloying and milling, Progress in materials science 46(1-2) (2001) 1-184.
[38] F.L. Zhang, C.Y. Wang, M. Zhu, Nanostructured WC/Co composite powder prepared by high energy ball milling, Scripta Materialia 49(11) (2003) 1123-1128.
[39] J. Safari, M.D. Chermahini, G. Akbari, The effect of Mg content on microstructure and mechanical properties of Al–xMg/5Al_2O_3 nanocomposite prepared by mechanical alloying, Powder technology 234 (2013) 7-12.
[40] K. Youssef, R. Scattergood, K. Murty, C. Koch, Nanocrystalline Al–Mg alloy with ultrahigh strength and good ductility, Scripta materialia 54(2) (2006) 251-256.
[41] J. Gubicza, M. Kassem, G. Ribárik, T. Ungár, The microstructure of mechanically alloyed Al–Mg determined by X-ray diffraction peak profile analysis, Materials Science and Engineering: A 372(1) (2004) 115-122.
[42] S. Scudino, M. Sakaliyska, K.B. Surreddi, J. Eckert, Mechanical alloying and milling of Al–Mg alloys, Journal of Alloys and Compounds 483(1-2) (2009) 2-7.
[43] F. Tarasi, M. Medraj, A. Dolatabadi, J. Oberste-Berghaus, C. Moreau, Amorphous and crystalline phase formation during suspension plasma spraying of the alumina–zirconia composite, Journal of the European Ceramic Society 31(15) (2011) 2903-2913.
[44] A. Simchi, S. Kamrani, S.M. Seyed Reihani, WITHDRAWN: Processing of Al-SiC nanocomposite powder by high-energy ball milling, Journal of Materials Processing Technology (2007).
[45] M.A. Baghchesara, H. Abdizadeh, H.R. Baharvandi, Effects of MgO Nano Particles on Microstructural and Mechanical Properties of Aluminum Matrix Composite prepared via Powder Metallurgy Route, International Journal of Modern Physics: Conference Series 05 (2012) 607-614.
[46] V.K. Dwivedi, S.P. Dwivedi, R. Yadav, Effect of heat treatment process on microstructure and mechanical behaviour of Al/MgO composite material, Advances in Materials and Processing Technologies (2020) 1-10.